

Primordial magnetic fields and formation of molecular hydrogen

Shiv K. Sethi¹, Biman B. Nath¹, Kandaswamy Subramanian²

¹*Raman Research Institute, Sadashivanagar, Bangalore 560080, India*

²*Inter-University Center for Astronomy & Astrophysics, Post Bag 4, Ganeshkhind, Pune 411007, India*
emails: sethi, biman@rri.res.in. kandu@iucaa.ernet.in

2 February 2022

ABSTRACT

We study the implications of primordial magnetic fields for the thermal and ionization history of the post-recombination era. In particular we compute the effects of dissipation of primordial magnetic fields owing to ambipolar diffusion and decaying turbulence in the intergalactic medium (IGM) and the collapsing halos and compute the effects of the altered thermal and ionization history on the formation of molecular hydrogen. We show that, for magnetic field strengths in the range $2 \times 10^{-10} \text{ G} \lesssim B_0 \lesssim 2 \times 10^{-9} \text{ G}$, the molecular hydrogen fraction in IGM and collapsing halo can increase by a factor 5 to 1000 over the case with no magnetic fields. We discuss the implication of the increased molecular hydrogen fraction on the radiative transfer of UV photons and the formation of first structures in the universe.

1 INTRODUCTION

It is believed that the first luminous objects in the universe appeared at $z \sim 15\text{--}30$ when substantial amount of molecular hydrogen formed in objects of mass $\simeq 10^{6-7} M_\odot$ (Tegmark et al. 1997). The first calculations of the production of H_2 by Saslaw & Zipoy (1967) had proposed that H_2 molecules formed through H_2^+ as an intermediate state, but Peebles & Dicke (1968) and Hirasawa et al. (1969) suggested that a more dominant intermediate state was the H^- ion. Subsequent calculations by Lepp & Shull (1984) showed that the intergalactic medium (IGM) would have a final H_2 abundance of $\simeq 10^{-6}$. Recently, Hirata & Padmanabhan (2006) showed the dominance of the H^- intermediate stage and calculated a final abundance of $\text{H}_2 \simeq 6 \times 10^{-7}$ in the intergalactic gas for the standard cosmology.

These calculations depend crucially on the residual ionization fraction of the universe after recombination. Recently, several authors have considered the effects of a primordial magnetic field, of order $\simeq 10^{-9} \text{ G}$ (in comoving frame), on the formation of large scale structure in the universe (Sethi & Subramanian 2005; Yamazaki et al. 2006a). The dissipation of primordial magnetic field energy is likely to raise the IGM temperature to $\simeq 10^4$ at redshifts $z \geq 100$, and collisional ionization in this gas is likely to increase the ionization fraction of the IGM much above the standard level of $\simeq 10^{-4}$ assumed in the calculations (of H_2 production) mentioned above (Sethi & Subramanian 2005). Here we consider the detailed chemistry of the production of H_2 molecule in the presence of dissipation of primordial magnetic field in the IGM. We also study the effect of magnetic field dissipation during the formation of H_2 molecules in the collapse of the first objects.

It is believed that these first luminous objects were instrumental in ushering the epoch of reionization, through UV photons radiating from the first generation stars in these objects. We know that the universe was reionized by $z \sim 6$ from Gunn-Peterson test of QSO absorption lines (see, e.g., Fan, Carilli & Keating 2006). Study of the anisotropy of cosmic microwave background (CMB) has put limits on the electron scattering optical depth in the IGM, which shows that the universe was reionized at $z \simeq 10$ (Spergel et al. 2006).

The presence of magnetic fields in the early universe can significantly change the standard history of star formation in the universe (Sethi and Subramanian 2005). They also showed that magnetic fields can seed early formation of structures, with collapse redshift almost independent of the strength of the magnetic field. Tashiro & Sugiyama (2005) considered several models of early reionization with primordial magnetic fields with magnetic fields strengths $\sim 10^{-9} \text{ G}$.

In this paper, we consider other important implications of primordial magnetic fields for the formation of first structures: (a) thermal and ionization history for collapsing haloes, and (b) the formation of molecular hydrogen.

In the next section, we discuss the relevant equations. In §3, we discuss the dissipation mechanisms of the magnetic field

energy. In §4, we present our results. The implications of the results for the formation of the first structures is discussed in §5. We summarize and conclude our findings in §6. Throughout this paper we use the FRW model favoured by the WMAP results (Spergel et al. 2007): spatially flat with $\Omega_m = 0.3$ and $\Omega_\Lambda = 0.7$ with $\Omega_b h^2 = 0.022$ and $h = 0.7$ (Freedman et al. 2001).

2 FORMATION OF MOLECULAR HYDROGEN

In the absence of dust grains, the formation of molecular hydrogen progresses through two channels— with either H^- or H_2^+ in the intermediate stage. In the first process the catalyst is an electron, which attaches to a neutral hydrogen atom radiatively to form H^- ,



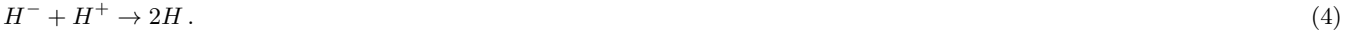
which goes to form H_2 molecule by the reaction:



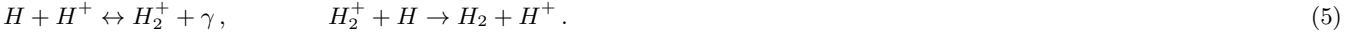
The H^- ion can be destroyed (or used up to produce something other than H_2) in two ways. It can be destroyed by energetic photons, mostly provided by the cosmic microwave background in the cosmological setting:



It can also combine with a proton in the following way:



The alternative channel through the formation of H_2^+ occurs when a proton acts as a catalyst:



There is also a third channel through the formation of HeH^+ . Recently, Hirata & Padmanabhan have shown that the H^- channel dominates the production of the H_2 molecule, with only $\sim 1\%$ contribution from the H_2^+ channel, and $\sim 0.004\%$ from the HeH^+ channel. We therefore use the H^- channel in our calculations, and the rate of formation of H^- is determined by,

$$\begin{aligned} \frac{dx[H^-]}{dt} = & k_1 x_e x_{HI} n_b - k_\gamma x[H^-] - k_2 x[H^-] x_{HI} n_b \\ & - k_3 x[H^-] x[H^+] n_b, \end{aligned} \quad (6)$$

Here x_e , x_{HI} , $x[H^-]$ are the ionized fraction, the neutral fraction, and the fraction of H-ion H^- , respectively; n_b is the total baryon density; k_1 is the rate for the reaction 1, k_2 is the rate of formation of H_2 in reaction 2, k_3 and k_γ are the rates of destruction of H^- in reactions 4 and 3. We use the fits in Stancil et al. (1998) for the first three rates:

$$\begin{aligned} k_1 &= 3 \times 10^{-16} \left(\frac{T}{300 \text{ K}} \right)^{0.95} \exp(-T/9320 \text{ K}) \text{ cm}^3 \text{ s}^{-1}, \\ k_2 &= 1.5 \times 10^{-9} \left(\frac{T}{300 \text{ K}} \right)^{-0.1} \text{ cm}^3 \text{ s}^{-1}, \\ k_3 &= 4 \times 10^{-8} \left(\frac{T}{300 \text{ K}} \right)^{-0.5} \text{ cm}^3 \text{ s}^{-1}. \end{aligned} \quad (7)$$

Following Hirata & Padmanabhan (2007), the rate of destruction by photons is taken as (for a blackbody spectrum of temperature T_{cbr}),

$$k_\gamma(T_{\text{cbr}}) = 4 \left(\frac{m_e k_B T_{\text{cbr}}}{2\pi \hbar^2} \right)^{3/2} \exp(-0.754 \text{ eV}/(k_B T_{\text{cbr}})) \times k_1(T_{\text{cbr}}), \quad (8)$$

where 0.754 eV is the photo-dissociation threshold energy for the H^- ion. We neglect the changes in the rate produced by any distortion of the microwave background radiation from a pure blackbody spectrum. These rates are faster than the Hubble rate of expansion for relevant epochs, so that one can write the steady-state abundance of H^- as,

$$x[H^-] = \frac{k_1 x_e x_{HI} n_b}{k_2 x_{HI} n_b + k_\gamma + k_3 x[H^+] n_b}. \quad (9)$$

Molecular hydrogen can be destroyed by electrons if the gas is significantly hotter than $\simeq 10^4 \text{ K}$;



We include this reaction since our calculation involves gas at high temperatures, with a rate adopted from Hirasawa (1969),

$$k_4 = 2.7 \times 10^{-8} T^{-3/2} \exp(-43,000 \text{ K}/T) \text{ cm}^3 \text{ s}^{-1}. \quad (11)$$

The rate of formation of molecular hydrogen is then given by,

$$\frac{dx[H_2]}{dt} = k_m n_b x_e (1 - x_e - 2x[H_2]) - k_4 n_b x_e x[H_2]. \quad (12)$$

where the rate of formation through the H^- stage is given by,

$$k_m = \frac{k_1 k_2 x_{HI} n_b}{k_2 x_{HI} n_b + k_\gamma + k_3 x[H^+] n_b}. \quad (13)$$

The first term in Eq (12) refers to the net rate of formation of H_2 through the H^- channel. The second term of Eq (12) refers to the direct destruction of H_2 by electrons with rate coefficient k_4 .

These equations must be supplemented by equations governing the density n_b and temperature T of the gas. For the case of IGM expanding with the Hubble rate, the particle density n_b is given by $n_b = n_0(1+z)^3$, where $n_0 = \rho_c(0)\Omega_b/(\mu m_p)$, where $\rho_c(0)$ is the critical density at present epoch, $\mu \simeq 1.22$ is the mean molecular weight for a fully neutral gas (the value relevant for us in this paper) and m_p is proton mass.

The equation determining the gas temperature is given by,

$$\frac{dT}{dt} = \frac{2}{3} \frac{n_b}{n_b} T + k_{iC} x_e (T_{\text{cbr}} - T) + \frac{2}{3 n_b k_B} (L_{\text{heat}} - L_{\text{cool}}), \quad (14)$$

where the first term describes adiabatic cooling (or heating), the second term refers to the inverse Compton cooling (or Compton heating), and L_{heat} , L_{cool} are other heating and cooling (volume) rates. We use,

$$k_{iC} = \frac{4\pi^2}{15} \left(\frac{k T_{\text{cbr}}}{\hbar c} \right)^4 \frac{\hbar \sigma_T}{m_e} = 2.48 \times 10^{-22} T_{\text{cbr}}^4 \text{ s}^{-1}. \quad (15)$$

The other important source of cooling apart from the Compton cooling is the HI line cooling with (e.g. Cen 1992):

$$L_{\text{cool}} = 7.9 \times 10^{-19} \left(1 + \left(\frac{T}{10^5 \text{ K}} \right)^{0.5} \right)^{-1} \times \exp(-118348/T) x_e x_{\text{HI}} n_b \text{ erg s}^{-1} \quad (16)$$

The HI line cooling is important when the temperature of the collapsing halo exceeds temperatures $\gtrsim 10^4 \text{ K}$. The heating term in Eq. (14) is given by the dissipation of primordial magnetic field energy and is discussed in the next section.

The evolution of the ionized fraction is given by:

$$\dot{x}_e = [\beta_e (1 - x_e) \exp(-h\nu_\alpha/(k_B T_{\text{cbr}})) - \alpha_e n_b x_e^2] C + \gamma_e n_b (1 - x_e) x_e \quad (17)$$

In this equation, the first two terms are the terms for the recombination of the primeval plasma (for details and notation see Peebles 1968, Peebles 1993). For $z \lesssim 800$, $C \simeq 1$ and the first term on the right hand of the equation rapidly decreases. After the recombination is completed, the only important term is the recombination term (the second term on the right hand side) which gives a slow decrease in the ionization fraction. The third term on the right hand side of the equation corresponds to the collisional ionization of the IGM. This term is expected to play an important role in partially ionizing the IGM owing to the dissipation of magnetic field energy since the temperature may become comparable to 10^4 K in many cases.

For an overdense region collapsing to virialise at a certain redshift z_{vir} , we calculate the density from the equation of motion of a bound shell collapsing under gravity (for details see e.g. Padmanabhan 1993, Peebles 1980):

$$\ddot{r} = -\frac{GM}{r^2} \quad (18)$$

(ignoring the effect of cosmological constant at high redshift). The parametric solutions of this equation are given by:

$$\begin{aligned} r &= 2r_{\text{vir}}[(1 - \cos \theta)/2], \\ t &= t_c[(\theta - \sin \theta)/2\pi], \end{aligned} \quad (19)$$

Here, t_c is the age of the universe at the collapse redshift z_{vir} , and $r_{\text{vir}} = r_{\text{max}}/2 = \frac{1}{2}[(2GMt_c^2)/\pi^2]^{1/3}$ is the radius at virialization. The density is assumed to be constant after virialization, given by the mean overdensity $\sim 18\pi^2$ expected in the spherical top-hat model. In this case, the gas density first decreases due to universal expansion, and then slowly increases prior to the collapse redshift to reach an overdensity of $18\pi^2$ at z_{vir} . The corresponding increase in temperature from adiabatic compression is given by the first term of equation 14. The final temperature reached by the gas after virialization depends on the mass of the object, M , through the virial condition:

$$T_{\text{vir}} \simeq 800 \text{ K} \left(\frac{M}{10^6 M_\odot} \right)^{2/3} \left(\frac{1+z}{20} \right) \left(\frac{\Omega_m}{0.3} \right)^{1/3} \left(\frac{h}{0.7} \right)^{2/3} \left(\frac{\mu}{1.22} \right). \quad (20)$$

3 PRIMORDIAL MAGNETIC FIELDS AND ENERGY DISSIPATION IN THE POST-RECOMBINATION ERA

Next, we discuss the importance of primordial tangled magnetic field for the production of molecular hydrogen. Primordial tangled magnetic fields can play an important role in the formation of structures in the universe. In particular, they can lead to early formation of structures and leave detectable traces in the CMBR temperature and polarization anisotropies (e.g. Barrow, Ferreira & Silk 1997; Subramanian & Barrow 1998a, 1998b; Durrer, Ferreira, Kahniashvili, 2000; Seshadri & Subramanian 2001; Caprini & Durrer 2002; Subramanian, Seshadri & Barrow 2003; Lewis 2004, Gopal & Sethi 2003, 2005; Yamazaki, Ichiki, & Kajino 2005, Yamazaki et al. 2006b, Wasserman 1978, Giovannini 2006).

Sethi and Subramanian (2005) studied the effects of the dissipation of magnetic field energy owing to ambipolar diffusion and decaying turbulence in the post-recombination era. In particular they showed that for magnetic field strengths $\simeq 3 \times 10^{-9}$ G this dissipation can result in thermal and ionization history substantially different from the usual case.

Here, we also generalize the analysis of Sethi and Subramanian (2005) to take into account the effects of this dissipation in a spherically collapsing halo. Our main aim here is to study the effects of this dissipation on the formation of molecular hydrogen in the background IGM and also in a collapsing halo. The magnetic field energy dissipation owing to ambipolar diffusion can be expressed as (see e.g. Cowling (1956), Shu (1991)):

$$\left(\frac{dE_B}{dt}\right)_{\text{ambi}} = \frac{\rho_n}{16\pi^2\gamma\rho_b^2\rho_i} |(\nabla \mathbf{x} \mathbf{B}) \mathbf{x} \mathbf{B}|^2 \quad (21)$$

Here ρ_n , ρ_b , and ρ_i correspond respectively to the neutral, total, and ionized mass density; $\gamma = \langle w\sigma_{\text{in}} \rangle / (m_n + m_i)$ (Shu 1992), where w is the ion-neutral relative velocity and σ_{in} is the cross section for the collision between ions and neutrals. For $w \lesssim 10 \text{ km sec}^{-1}$, $\langle w\sigma_{\text{in}} \rangle \simeq 3 \times 10^{-9} \text{ cm}^3 \text{ sec}^{-1}$ independent of the relative velocity of ions and neutrals. We use this value throughout as it is a valid approximation in our case. We assume the tangled magnetic field to be statistically homogeneous and isotropic and Gaussian with a power spectrum: $M(k) = Ak^n$ with a large- k cut off at $k = k_{\text{max}}$; k_{max} is determined by the effects of damping by radiative viscosity during the pre-recombination era (Jedamzik, Katalinić, & Olinto 1998, Subramanian & Barrow 1998b; for more details see also Sethi and Subramanian 2005). The normalization A can be determined by smoothing the magnetic field over a given scale k_G . We continue to refer to the RMS of the tangled magnetic field smoothed over this scale (with a sharp k -space filter) with $k_G = 1 \text{ Mpc}^{-1}$ as the magnetic field strength, B_0 . We assume the magnetic field power spectrum to be nearly scale invariant with, $n \simeq -3$, for our study. Many theoretical analyzes show that these are the only power spectra compatible with current observations (e.g. Caprini & Durrer 2002, Sethi and Subramanian 2005 and references therein). For obtaining numerical results, we use $n = -2.8$ throughout this paper. Also, for these spectra, the RMS is not sensitive to the exact choice of the smoothing scale.

In linear theory, it results in the flux freezing condition $Ba^2 = \text{const}$, where a is the scale factor of the expanding universe. Using this, the magnetic field term in the above expression can be simplified to (for details see Sethi and Subramanian (2005)):

$$\left\langle [(\nabla_{\mathbf{x}} \times \tilde{\mathbf{B}}) \times \tilde{\mathbf{B}}]^2 \right\rangle = \frac{7}{3} \int dk_1 \int dk_2 M(k_1) M(k_2) k_1^2 k_2^4 \quad (22)$$

Here x refers to comoving coordinates and $\tilde{\mathbf{B}} = \mathbf{B}a^2$ is the value of the magnetic field at the present epoch. The expression given above is exact in linear perturbation theory. For taking into account the formation of non-linear structures, we continue to use the flux-freezing condition and generalize it to: $Bn_b^{2/3} = \text{const}$ and allow the comoving length (constant in linear theory) to be $\propto [n_b^{1/3}(1+z)]^{-1}$.

Magnetic field energy can also dissipate by generating decaying MHD turbulence. Sethi and Subramanian (2005) modelled this dissipation owing to MHD turbulence based on large scale simulation of this phenomenon in flat space. The simulations show that, the decay of magnetic field can be modelled as (see e.g. Banerjee & Jedamzik 2003, Christensson, Hindmarsh & Brandenburg 2001, Biskamp & Müller 2000):

$$\mathcal{E}_B = \frac{\mathcal{E}_{B0}}{(1 + \tilde{t}/\tilde{t}_d)^m}. \quad (23)$$

Here \tilde{t} is the time in 'flat-space', \tilde{t}_d is the relevant dynamical time for decay, and \mathcal{E}_B is the magnetic energy in flat space, with \mathcal{E}_{B0} its initial value. As discussed in Sethi and Subramanian (2005), the decaying turbulence sets in as the radiative viscosity drops rapidly during the recombination era. For our computation, we assume the decaying turbulence to set in at $z = 1000$, and therefore the initial magnetic field energy \mathcal{E}_{B0} is computed at this redshift. A change in the choice of initial redshift value doesn't make any essential difference to our results as the initial phase of dissipation is always logarithmic (to be discussed below). Simple scaling arguments suggest $m = 2(n+3)/(n+5)$, for an initial power spectrum with $n \gtrsim -3$ (cf. Olesen 1997, Shiromizu 1998, Christensson, Hindmarsh & Brandenburg 2001, Banerjee & Jedamzik 2003). This flat space result can be mapped to the case of expanding universe by using the following transformation of MHD equations (Banerjee & Jedamzik 2004):

$$\tilde{\mathbf{B}} = \mathbf{B}a^2, \quad d\tilde{t} = dt/a^{3/2}, \quad \tilde{v} = a^{1/2}v, \quad \tilde{\rho} = \rho a^3, \quad \tilde{p} = pa^4, \quad \tilde{\epsilon} = a^4\epsilon \quad (24)$$

For our study, the most important transformation concerns the transformation of time. As was shown in Sethi and Subramanian (2005), this means that a power-law dissipation in flat space translates to a logarithmic decay in the expanding universe. We generalize this concept to a collapsing halo here. Following Sethi and Subramanian (2005), the rate of dissipation of magnetic field energy owing to decaying turbulence can be expressed as:

$$\left(\frac{dE_B}{dt}\right)_{\text{turb}} = m \frac{B^2(t)}{8\pi} \frac{d\tilde{t}}{dt} \frac{1}{\tilde{t}_d} \frac{1}{(1 + \tilde{t}/\tilde{t}_d)} \quad (25)$$

For a collapsing halo, the transformation between \tilde{t} and t (Eq. (24)) can be computed by replacing the scale factor by the comoving length of the collapsing object. From Eq. (24), it can readily be shown that the dissipation in a collapsing halo is generally a power law and the dissipation of the magnetic field energy in a collapsing halo is generally more rapid. The evolution of magnetic field energy density can be written as:

$$\frac{dE_B}{dt} = \frac{4}{3} \frac{\dot{\rho}}{\rho} \left(\frac{dE_B}{dt}\right)_{\text{turb}} - \left(\frac{dE_B}{dt}\right)_{\text{ambi}} \quad (26)$$

The first term on the right hand side takes into account the change in the magnetic field energy owing to adiabatic expansion (in the early stages of the evolution of a halo) and compression (during the halo collapse). The heating terms in Eq. (14) correspond to:

$$L_{\text{heat}} = \left(\frac{dE_B}{dt}\right)_{\text{turb}} + \left(\frac{dE_B}{dt}\right)_{\text{ambi}} \quad (27)$$

4 RESULTS

The ionization and thermal history for several values of magnetic field strengths are shown in Figure 1 and 2 (the virial redshift $z_{\text{vir}} = 10$ for all the figures in the paper unless specified otherwise). The dissipation of magnetic field energy is seen to have significant effect on the thermal and ionization history in the post-recombination era. The more interesting case is the case of a collapsing halo. In this case, the magnetic field strength increases owing to the flux freezing condition as the halo starts collapsing, which also leads to an increase in the amount of magnetic field energy that is dissipated as more magnetic field energy becomes available. During the collapse phase, the heating mechanism of the halo is provided by both the adiabatic compression as well as the magnetic field energy dissipation. The main cooling mechanism for halos that exceed temperatures $\gtrsim 10^4$ K is the HI line cooling and this prevents the halo to reach temperatures much higher than this value, as is also seen in Figure 2.

We do not include here the temperature increase owing to the process of the virialization of the halo. This final increase in a collapsing halo depends on the mass of the halo as obtained by the virialization condition (Eq. (20)). The temperature histories we present for collapsing halos, however, do not depend on the mass of the halo but only on the strength of the magnetic field. This requires one to interpret the virialization condition differently. In the usual case without magnetic fields, the temperature reached by a collapsing halos (of mass scales of interest $\gtrsim 10^5 M_{\odot}$) owing to adiabatic compression is generally much lower than given by the virialization condition; this is because the final density is, as discussed above, roughly $18\pi^2$ times the IGM density, which gives the final temperature owing to adiabatic compression: $T_f \simeq (18\pi^2)^{2/3} T_{\text{IGM}}$. In our case, however, the temperature reached owing to magnetic field energy dissipation coupled to adiabatic collapse is far higher than this, and it is quite comparable to virial temperature of halos of mass scales of interest.

We therefore interpret the final temperature (T_f) reached by a halo to correspond to the virial temperature ($T_v(M)$) of the appropriate mass scale. This means that halos of smaller masses (with $T_v(M) < T_f$) cannot collapse gravitationally (or will evaporate during the collapse process) for the corresponding value of the magnetic field. For larger masses, the virialization process can raise the temperature of the halo above the value we obtain for a given value of magnetic field strength ($T_f > T_v(M)$). The line cooling, however, prevents the the temperature of the halo from rising above a value $\simeq 10^4$ K, as seen in Figure 2.

The virial temperature defined in this way is related to the usual Jeans' criterion. Given the density and temperature evolution of the gas, the Jeans' criterion can be expressed as a lower limit on the mass that is unstable to gravitational collapse, with this lower limit given by:

$$M \geq M_J = \frac{4\pi^4 c_s^3}{3(4\pi G)^{3/2} \rho_m^{1/2}} \quad (28)$$

Here $c_s^2 = (5/3)KT/(\mu m_p)$ is the square of sound speed at constant entropy.

4.1 Molecular hydrogen in the IGM

The rate of molecular hydrogen formation is a fairly sensitive function of the ionization fraction in the IGM (or collapsing halo) (see e.g. Tegmark et al. 1997). Owing to the dissipation of magnetic field energy, the IGM temperature is much higher than

in the usual case, and consequently, the ionization fraction in the IGM is much higher than the usual case, as seen in figure 1 and 2. The rate of molecular hydrogen formation increases as ionization fraction increases. However, a rise in temperature also increases the rate of destruction of H^- which is the intermediate product for the formation of the molecular hydrogen. It is an interplay of these two opposing effects that determines the production of molecular hydrogen in the presence of primordial magnetic field energy dissipation.

In Figure 3, we show the evolution of molecular hydrogen formation for several values of the primordial magnetic field. As seen in the Figure, the molecular hydrogen fraction is generally seen to increase with the strength of magnetic field. This shows that of the two opposing influences, the rise in the ionization level owing to magnetic field energy dissipation predominates in determining the production rate of molecular hydrogen. The dissipation of tangled magnetic field energy in the post-recombination era can, therefore, play a very important role in determining the formation of molecular hydrogen. As seen in Figure 3, the fraction of molecular hydrogen in the IGM can increase by more than two orders of magnitude owing to this process, for magnetic field strength $\simeq 3 \times 10^{-9}$ G. This can have several important implications for the formation of structures in the early universe and also the radiation transfer of UV light in the early universe. We discuss it in more detail in a later section.

4.2 Molecular hydrogen in collapsing haloes

In Figure 3 we show the molecular hydrogen fraction in collapsing haloes for many different values of the magnetic field. It is seen that, as in the usual case without magnetic field, the fraction of molecular hydrogen increases rapidly during the final collapse phase of the halo. However, as Figure 3 shows, the increase in molecular hydrogen fraction in the pre-collapse phase in the presence of magnetic fields is also quite important and might be primarily responsible for the increase in the fraction of molecular hydrogen as the magnetic field value is increased. In addition, as seen in Figure 1, the final collapse phase could be accompanied by an increase in the ionized fraction in the presence of magnetic fields, unlike the usual case; this leads to a further increase in the molecular hydrogen fraction. This suggests that the increase in molecular hydrogen fraction is determined by the entire ionization and thermal history in the presence of magnetic fields. For magnetic fields strengths of $B_0 \gtrsim 2.5 \times 10^{-10}$ G, the final abundance of molecular hydrogen fraction could reach values $\simeq 10^{-3}$ – 10^{-2} .

5 DISCUSSION

The possibility of increased abundance of H_2 in the IGM and the collapsing halos has important implications for the evolution of luminous structures in the universe.

In the usual case without magnetic fields, the smallest mass haloes (above the thermal Jeans mass $\simeq 10^5 M_\odot$) that satisfy the criterion for star formation ($t_{\text{cool}} \leq t_{\text{dyn}}$) can only cool by molecular hydrogen (e.g. Tegmark et al. 1997, for a review see Barkana & Loeb 2001). These first haloes are generally believed to have masses $\gtrsim 10^7 M_\odot$. However, there are two difficulties in forming and sustaining star-formation using H_2 -cooled haloes: (a) the cooling time t_{cool} depends directly on the abundance of molecular hydrogen fraction. In the usual case the fraction of molecular hydrogen is small $\simeq 2 \times 10^{-4}$, which barely meets the condition for runaway collapse of haloes owing to H_2 cooling. (b) Even if the first stars could form, the UV light from these first object can easily penetrate the surrounding IGM and destroy the H_2 in the neighboring haloes (Haiman, Rees, & Loeb 1997) thereby inhibiting further star-formation. The scenario in the presence of magnetic fields can obviate both these difficulties but it also introduces additional complications.

The introduction of magnetic field energy dissipation is seen to increase the molecular hydrogen fraction by up to two orders of magnitude (Figure 3). This decreases the cooling time of the collapsing halo and would seem to suggest that haloes would not only collapse more readily but haloes of a wider set of masses would now become unstable to collapse. However, this is not the case owing to two reasons: (a) as discussed above, the temperature reached in the collapsing haloes are higher owing to the magnetic field energy dissipation. If this temperature exceeds the thermal Jeans' mass (Eq. (28)) then the halo cannot collapse, (b) haloes of masses smaller than magnetic Jean's mass cannot collapse (for details of structure formation in the presence of magnetic fields see e.g. Sethi and Subramanian 2005 and discussion below).

In Figure 4, we show the minimum thermal Jeans' mass (obtained from the condition given by Eq. (28)) and the magnetic Jeans' mass as a function of the magnetic field strength. The magnetic Jeans' mass is given by (see .e.g. Sethi & Subramanian 2005):

$$M_J^B \simeq 10^{10} M_\odot \left(\frac{B_0}{3 \times 10^{-9} \text{ G}} \right)^3. \quad (29)$$

The haloes of masses that lie in the range above both the curves shown in the figure can gravitationally collapse.

Some notable features of Figure 4 and their implications are: (a) magnetic Jeans's mass exceeds the thermal Jeans' mass for magnetic field strengths $\lesssim 10^{-10}$ G and $\gtrsim 10^{-9}$ G. (b) there exists a mass range $10^6 \lesssim M \lesssim 10^8 M_\odot$, which is Jeans' unstable according to both thermal and magnetic criteria. For a part of this mass range the magnetic field strength is between

roughly $2-4 \times 10^{-10}$ G. For these magnetic field strengths, as follows from Figure 3, the molecular hydrogen fraction in the collapsing halos could be in the range $1-5 \times 10^{-3}$, which is more than ten times higher than the usual case (see e.g. Tegmark et al. 1996). Therefore, the net effect of primordial magnetic field is to increase the molecular hydrogen fraction in an interesting range of masses. And the main implication of this increase is to increase the cooling efficiency and therefore the rate of collapse of these haloes. It also follows from Figure 3 and 4, that haloes with higher molecular hydrogen ($\gtrsim 0.01$) have masses $> 10^8 M_\odot$; these haloes, inspite of having higher molecular fraction, cool faster by atomic cooling (e.g. Barkana & Loeb 2001, Sethi 2005).

Sethi and Subramanian (2005) showed that primordial magnetic fields can induce early formation of structures. In particular they showed that for magnetic-field induced structure formation: (i) the mass dispersion $\sigma_B(R)$ could reach values large enough to cause a $1-\sigma$ collapse at high redshifts; the value of collapse redshift is only sensitive to the magnetic field spectral index and not its strength (provided $M > M_J$) (ii) $\sigma_B(R) \propto 1/R^2$, or the mass dispersion decreases quite rapidly with the mass scale and therefore most of collapsed structures would have masses close to the magnetic Jeans' mass. The magnetically-induced structure formation is in addition to the structure formation in the usual Λ CDM model. The mass dispersion at any scale in the presence of primordial magnetic field is: $\sigma(R) = \sqrt{\sigma_{\Lambda\text{CDM}}^2 + \sigma_B^2}$. These conclusions can be suitably revised in the light of results shown in Figure 4.

Sethi and Subramanian (2005) (Figure 7) showed that for magnetic field spectral index $n = -2.8$, $\sigma_B \simeq 1.5$ at the scale of magnetic Jeans' length, at $z \simeq 10$. This means that at this redshift a $1-\sigma$ density perturbation can collapse. It follows from Figure 4, that for magnetic field strength $B_0 \lesssim 10^{-9}$, it is usually the thermal Jeans' mass that is important for the collapse criterion. For example, for $B_0 \simeq 4 \times 10^{-10}$ G, the thermal Jeans' mass is roughly a factor of a factor of 5 greater than the magnetic Jeans' mass; the mass dispersion at this scale is roughly 0.8, which means only a $2-\sigma$ perturbation can collapse. This is in addition to Λ CDM model-induced perturbations. The collapse of these perturbations is not changed much by the increase in Jeans' length shown in Figure 4 because $\sigma_{\Lambda\text{CDM}}$ is roughly independent of scale at small scales (scales corresponding to $M \lesssim 10^8 M_\odot$). From WMAP-normalized $\sigma_{\Lambda\text{CDM}}$ power spectrum, $\sigma_{\Lambda\text{CDM}}$ at scales under discussion is $\simeq 0.7$, which means a $2.5-\sigma$ perturbation can result in collapsed structures.

For magnetic field spectral index $n = -2.9$, $\sigma_B \simeq 0.5$ at the scale of magnetic Jeans' length, at $z \simeq 10$ (Figure 7, Sethi and Subramanian 2005). This means magnetic field-induced structure formation is not as dominant as the Λ CDM model. The thermal history of the universe owing to magnetic field energy dissipation and its implications, as presented here, are not sensitive to the value of n . Therefore, the main effect of the presence of primordial magnetic fields for $n \lesssim -2.9$ is to alter the thermal history and the H_2 formation in the universe. However, magnetically-induced structure formation would also be important for larger values of n .

As mentioned above, the formation of structures with H_2 -cooled haloes is self-inhibiting owing to the destruction of H_2 by the UV photons emitted by first objects. This is because IGM is optically thin to the UV photons in the Lyman-Werner (LW) band (11.8–13.6 eV). In the usual case, the abundance of H_2 in the IGM is $\simeq 10^{-6}$ and the photons emitted by first generation (Population III) stars in the Lyman-Werner band are absorbed to some extent by the H_2 molecule in the IGM. These photons, if unabsorbed, can photodissociate H_2 molecule in neighbouring objects. This phenomenon may cause a decrease in the star formation rate in the universe, until more massive objects form through atomic cooling begin to appear in abundance, or enough H_2 molecule has form by the influence of ionization from X-ray photons which may be present (Haiman, Abel, Rees 2000; Glover, Brand 2003).

Haiman, Abel and Rees (2000) estimated that for an abundance of $\simeq 2 \times 10^{-6}$ in the IGM, the opacity of LW band photons can be as large as $\simeq 0.2$ at $z \simeq 15$. As discussed by Cen (2003), the efficacy of LW photons in dissociating H_2 molecule—which competes with production of H_2 molecules with the help of free electrons generated by higher energy photons—can be described by a ratio $\psi \sim E_{\text{LW}}/E_{>1\text{ keV}}$. Consider a background radiation with spectrum $J_\nu \propto \nu^{-1}$, as considered by Haiman et al (2000). Cen (2003) summarized the results of Haiman et al (2000) (which had likely underestimated the opacity of LW photons by a factor $\simeq 6$ (Cen 2003)) to state that the destruction of H_2 molecules by LW bands is compensated by production of H_2 molecules owing to ionization by higher energy photons, if $\psi \leq 5$. Typically, for Population III stars Cen (2003) estimated the ratio to be $\psi \sim 2.5$.

The opacity of LW photons scales linearly with the H_2 molecule abundance. Therefore, if the IGM abundance of H_2 molecule increases even by a factor $\simeq 5-30$ (which corresponds to a magnetic field of order $\simeq 4 \times 10^{-10}$ G, from Figure 3), the opacity of LW band photons can be large enough to block them from destroying H_2 molecule in nearby objects. In this case, the star formation history is likely to be less affected by the UV emission of Population III stars than in the usual case. Therefore, the presence of tangled primordial magnetic field in the IGM can have substantial effect in the history of star formation in the universe.

6 SUMMARY AND CONCLUSIONS

In this paper, we explored the implications of the presence of primordial magnetic fields on the formation of molecular hydrogen in the first collapsed objects in the universe.

We showed that the dissipation of the primordial magnetic field energy in the post-recombination era can alter the ionization and thermal evolution substantially. The net effect of this change is to increase the molecular hydrogen abundance by many orders of magnitude, depending on the value of the magnetic field.

We discuss how the increase in the molecular hydrogen abundance can have a direct bearing on the formation and survival of the first objects. The net impact of the primordial magnetic fields depends also on the role played by the magnetic fields in inducing the formation of first structures.

In future, we hope to explore the observational consequences of the effects of primordial magnetic fields in the formation of the first structures in the universe.

ACKNOWLEDGMENT

We would like to thank Zoltan Haiman for providing data on the absorption of UV photons in the Larmer-Werner band. We also thank S. Sridhar for fruitful discussion.

REFERENCES

- Banerjee, R. & Jedamzik, K. 2003, Physical Review Letters, 91, 251301-1
 Banerjee, R. & Jedamzik, K. 2004, Phys. Rev. D, 72, 123003-1
 Barkana, R. and Loeb, A. 2001, Phys. Rep., 349, 125
 Barrow, J. D., Ferreira, P. G., & Silk, J. 1997, Physical Review Letters, 78, 3610
 Caprini, C. & Durrer, R. 2002, Phys. Rev. D, 65, 023517
 Cen, R. 2003, ApJ, 591, 12
 Cen, R. 1992, ApJS, 78, 341
 Christensson, M., Hindmarsh, M., & Brandenburg, A. 2001, Phys. Rev. E, 64, 56405
 Cowling, T. G. 1956, MNRAS, 116, 114
 Durrer R., Ferreira P. G., Kahnashvili T., 2000, Phys. Rev. D, 61, 043001
 Fan, X, Carilli, C. L., Keating, B. 2006, ARAA, 44, 415
 Freedman, W. L. et al. 2001, ApJ, 553, 47
 Giovannini, M. 2006, Phys. Rev. D., 74, 3002
 Gopal, R. & Sethi, S. K., 2003, Journal of Astrophysics and Astronomy, 24, 51
 Haiman, Z., Rees, M. & Loeb, A. 1997, ApJ, 476, 458
 Haiman, Z., Abel, T., Rees, M. J. 2000, ApJ, 534, 11
 Hirasawa, T. 1969, Prog. Theor. Phys., 42, 523
 Hirata, C., Padmanabhan, N. 2006, MNRAS, 372, 1175
 Jedamzik, K., Katalinić, V., & Olinto, A. V. 1998, PRD, 57, 3264
 Lepp, S., Shull, J. M. 1984, ApJ, 280, 465
 Lewis, A. 2004, Phys. Rev. D, 70, 43011
 Müller, W. & Biskamp, D. 2000, Physical Review Letters, 84, 475
 Olesen, P., 1997, Phys. Lett., B398, 321
 Padmanabhan, T. 1993, Cambridge, UK: Cambridge University Press
 Peebles, P. J. E. 1993, Principles of Physical Cosmology, Princeton University Press
 Peebles, P. J. E. 1980, The Large Scale Structure of the Universe, Princeton University Press
 Peebles, P. J. E. 1968, ApJ, 153, 1
 Saslaw, W. C., Zipoy, D. 1967, Nature, 216, 976
 Seshadri, T. R. & Subramanian, K. 2001, Physical Review Letters, 87, 101301
 Sethi, S. 2005, Current Science, 88, no. 7
 Sethi, S., Subramanian, K. 2005, MNRAS, 356, 778
 Shiromizu, T., 1998, Phys. Lett., B443, 127
 Spergel, D. N. et al, 2007, ApJS, 170, 377
 Stancil, P. C., Lepp, S., Dalgarno, A. 1998, ApJ, 509, 1
 Shu, F. H. 1992, Gas Dynamics, University Science Books
 Subramanian, K., Seshadri, T. R., & Barrow, J. D. 2003, MNRAS, 344, L31
 Subramanian, K. & Barrow, J. D. 1998a, Physical Review Letters, 81, 3575
 Subramanian, K. & Barrow, J. D. 1998b, PRD, 58, 83502
 Tashiro H., Sugiyama, N. 2006, MNRAS, 368, 965
 Tegmark, M., Silk, J., Rees, M. J., Blanchard, A., Abel, T., Palla, F. 1997, ApJ, 474, 1
 Wasserman, I. 1978, ApJ, 224, 337
 Yamazaki, D. G., Ichiki, K., Umezu, K., Hanayana, H. 2006a, PRD, 74, 13518
 Yamazaki, D. G., Ichiki, K., Kajino, T., Mathews, G. J. 2006b, ApJ, 646, 719

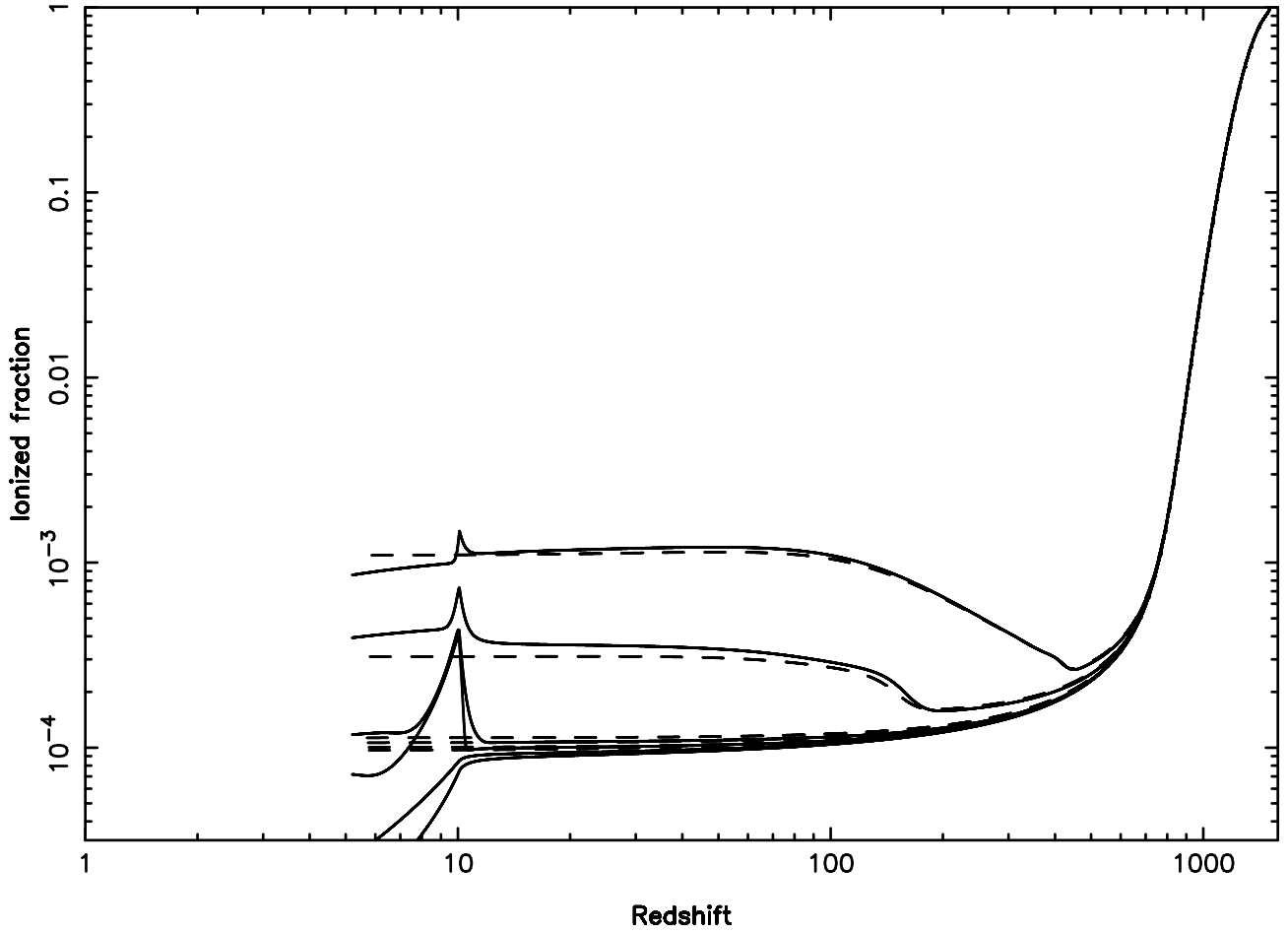


Figure 1. The ionized history is shown for the IGM (dashed lines) and a collapsing haloes (solid curves) for several different choices of the magnetic field strength. The different curves (from bottom up) correspond to magnetic field strengths: $\{10^{-10}, 2.5 \times 10^{-10}, 3.5 \times 10^{-10}, 6 \times 10^{-10}, 10^{-9}, 3 \times 10^{-9}\}$ G.

Yamazaki, D. G., Ichiki, K., Kajino, T. 2005, ApJ, 625, L1

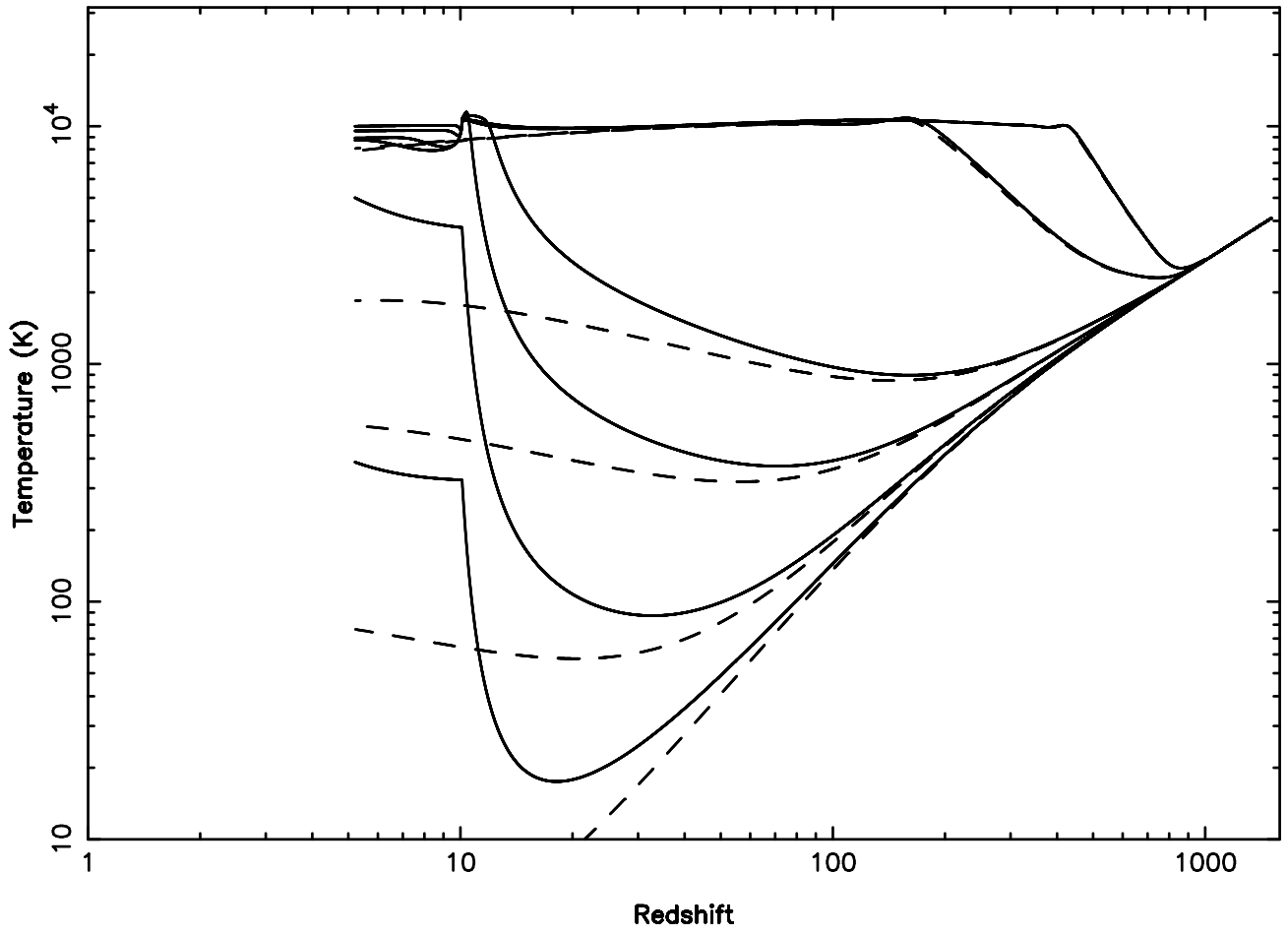


Figure 2. The thermal history of IGM and collapsing halo is shown. The parameters and the plotting style is the same as Figure 1

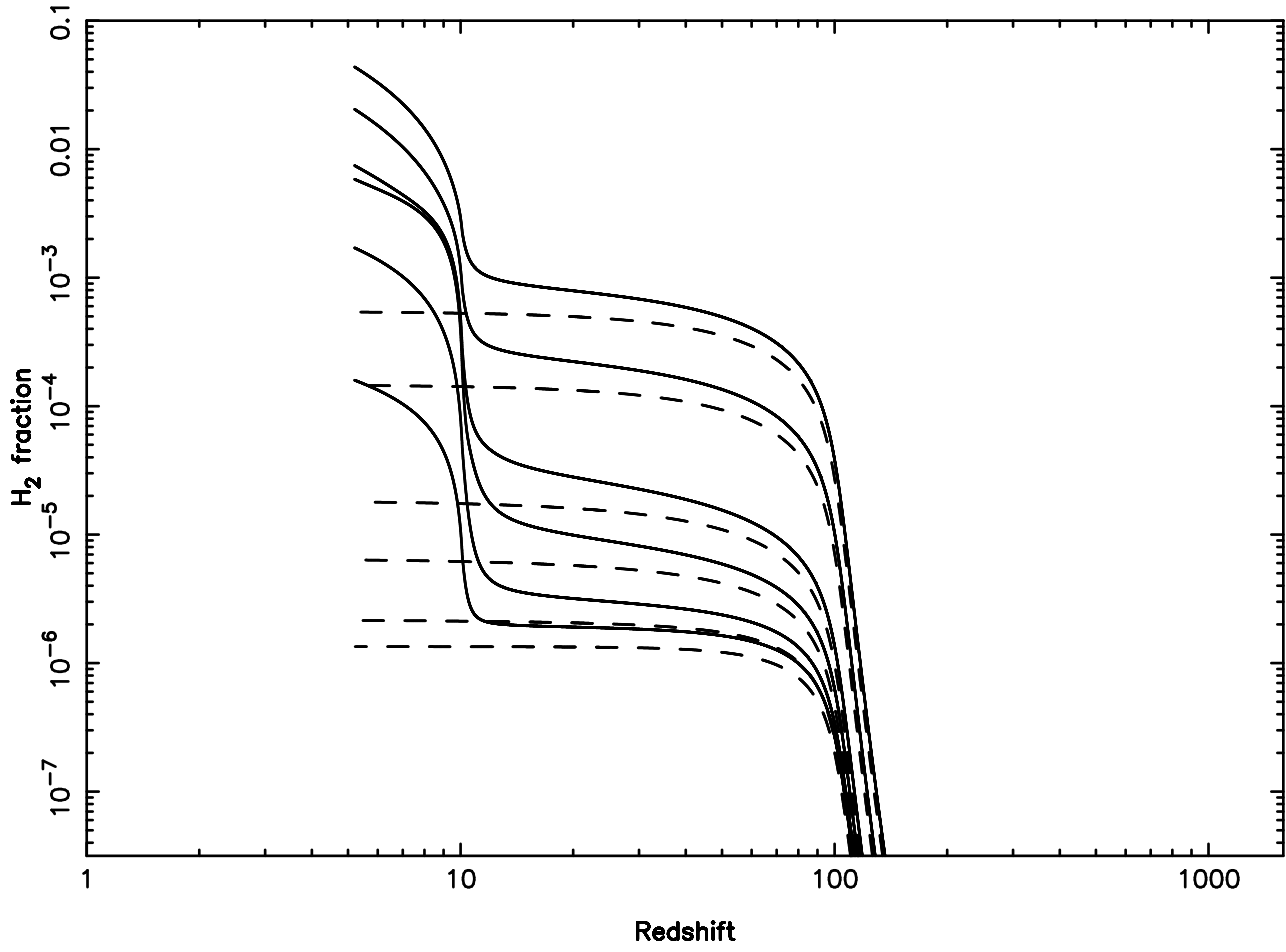


Figure 3. The molecular hydrogen fraction in IGM and collapsing halos is shown. The parameters and the plotting style is the same as Figure 1

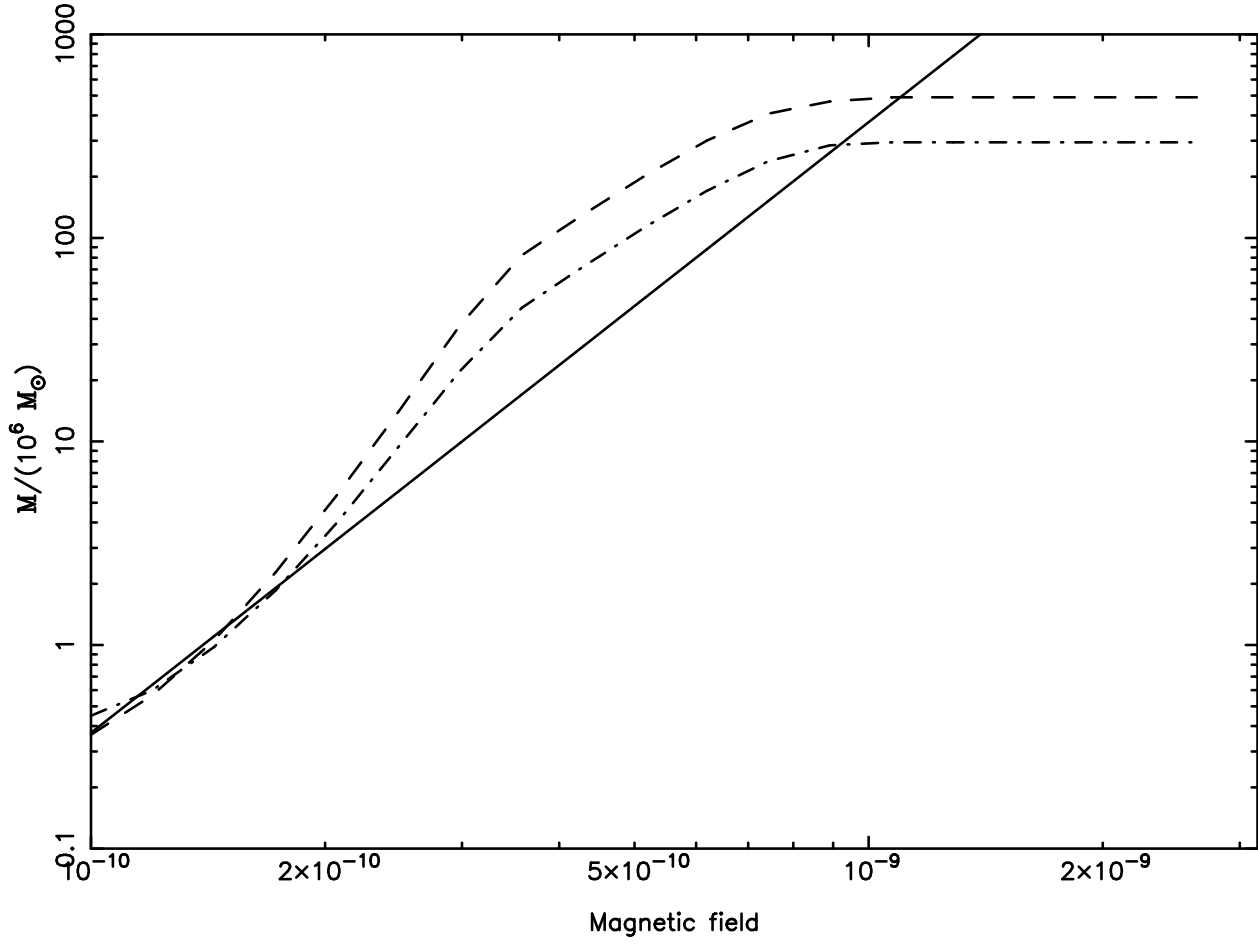


Figure 4. The solid curve shows the magnetic Jeans mass as a function of Magnetic field strength. The dashed curves, top to bottom, are obtained by the condition given by Eq. (28) for $z_{\text{vir}} = \{10, 15\}$, respectively.